

SUPPLEMENTARY METHODS AND FIGURES

Supplementary Methods

Human ovarian and colon tumor collection

High-grade serous ovarian carcinoma tissue from five patients was collected as previously reported (1). Colon adenocarcinoma biopsy tissue was collected from five patients at the Cooperative Human Tissue Network at Vanderbilt University Medical Centre (CHTN-VUMC), in accordance with IRB-approved protocols. All patients gave written informed consent prior to sample collection in accordance with existing CHTN-VUMC protocols. Following vessel ligation, surgical specimen removal was performed and the first core biopsy was taken immediately thereafter (t=0), transferred to prechilled cryovials and snap frozen in liquid nitrogen. The biopsy punch (4mm punch) was taken perpendicular to the resection margins to keep diagnostic areas of the total specimen intact. Further core biopsies were collected and frozen after 10, 30, and 60 minutes of cold ischemia. For each time point, cores punches were collected and split in half to yield 8 samples per tumor (i.e. 0_A, 0_B, 10_A, 10_B, 30_A, 30_B, 60_A, 60_B). Punches for the 10, 30 and 60 min samples were taken adjacent to prior timed punches on the specimen. The remaining total specimen underwent inspection in the surgical pathology suites for gross evaluation and histological quality control. Only specimens meeting pathology quality inclusion criteria of left sided colon adenocarcinoma cancers in which clamp time can easily be determined, minimal tumor diameter of 4 cm and no prior chemotherapy and/or radiation were released for analysis. All specimens were stored in -80°C freezers until shipment to MIT.

Phosphotyrosine data analysis

For each technical replicate (n=2) of an individual patient sample dataset, quantitative abundances of pTyr sites were computed by first subtotaling the iTRAQ reporter ion intensities from multiple detected scans of the same peptide. A relative fold change for a given iTRAQ channel was then expressed relative to the mean of all iTRAQ channels for that specific peptide (*i.e.* mean normalized 114= $114/(114+115+116+117)/4$). The normalized iTRAQ value was transformed to \log_2 scale. The final iTRAQ value for a given peptide was calculated from the mean of technical replicate measurements. For peptides detected in both technical replicates, the standard deviation (s.d.) and coefficient of variation (CV) of each iTRAQ value were calculated using each pair of replicate measurements. The average global technical error for each patient dataset was calculated as the mean CV from all replicate measurements in that patient dataset. This allowed an estimation of measurement error that could be attributed to technical variation.

Accordingly, pTyr temporal values ≥ 3 s.d away from the value at t=0 are considered greater than the global technical error and classified as 'changing'. The 'core' ischemia-regulated phosphorylation signature was identified and calculated as follows. First, for each patient pTyr sites were selected that showed temporal change (*i.e.* pTyr temporal values ≥ 3 s.d away from the value at t=0 are classified as 'changing'). pTyr sites within this subset that were detected in all five patients were selected. For these sites, the \log_2 deviation from t=0 at each timepoint and the absolute sum of these temporal deviations in each patient was calculated to quantify the magnitude of ischemia. A mean value for each pTyr site was computed from the absolute summed deviations in the 5 patients. The relative ischemia index is therefore, the mean deviation value and

categorized into one of 4 major pathways according to PhosphoSitePlus functional annotations. The total list of peptides and proteins identified and quantified can be found in **Supplementary Table 1, 2 and 4**. All mass spectra, in the original instrument vendor format, contributing to this study may be downloaded from: <https://cptac-data-portal.georgetown.edu/cptacPublic/>

Mass-spectrometry based protein expression analysis

Approximately 10% (~300 µg) of iTRAQ labeled peptides from each colorectal tumor pTyr IP supernatant was separated off-line on an Eclipse XDB C18 column from Agilent (150 mm × 4.6 mm column containing 5 µM particles) using an Agilent 1200 HPLC System. The sample was loaded onto the C18 column and separated on an 80 min gradient. Mobile phase flow rate was 1.0 mL/min and consisted of 0.1% heptafluorobutyric acid (HFBA) in water (A) and 100% methanol in 0.1% HFBA with a linear gradient profile as follows (minute:%B); 2:0, 72:100, 75:100, 76:0, 80:0. A total of 80 fractions were collected using an automated fraction collector, and subsequently concentrated before lyophilization. The 80 reverse phase fractions were resuspended with 0.1% formic acid and combined into 20 final fractions by non-contiguously pooling 4 fractions at a time (ie. fraction 1+21+41+61, etc). Each final fraction of 20 µL was diluted 1/10 with 0.1% formic and 1 µl (equivalent of ~500 ng total protein) was used. Each of the 20 final fractions underwent an independent LC-MS/MS analysis. Each fraction was subsequently separated by reverse phase UHPLC (Easy-nLC 1000, Thermo Scientific) over a 140 min gradient before nanoelectrospray directly into a Q-Exactive mass spectrometer (Thermo Scientific). Samples were loaded by autosampler onto a 6-cm self-packed C18 capillary precolumn (YMC-Waters 10 µm ODS-A, and PolyMicro

Technologies 100 μm i.d. x 360 μm i.d. column) inline with a self-packed C18 silica picofrit capillary column with integrated emitter tip (YMC-Waters 5 μm ODS-AQ, and Picofrit-New Objective 10 μm tip opening, 10 cm x 50 μm i.d.). Mobile phases consisted of 0.1% formic acid in water (A) and 80% acetonitrile in 0.1% formic acid (B) operated at 150 nL/min with a gradient profile as follows (minute:%B); 3:13, 110:42, 113:100, 120:100, 130:0, 150:0. The Q-Exactive mass spectrometer was operated in data-dependent mode acquiring HCD scans ($R=35,000$, 1×10^5 target ions) after each full MS scan ($R=70,000$, 3×10^6 target ions) for the top ten most abundant ions within the mass range of 350 to 2000 m/z. An isolation window of 2.0 Th was used to isolate ions prior to HCD. All HCD scans used a normalized collision energy of 32 and a maximum inject time of 300 ms. The dynamic exclusion time was set to 30 s and charge state screening was enabled to reject unassigned and singly charged ions.

Protein expression data analysis

Peptide and protein identification were performed with the Proteome Discoverer software (version 1.4; Thermo Scientific) using Mascot search engine (version 2.4.1, Matrix Science). MS/MS spectra were searched against a human protein sequence database (NCBI nr, 2012 release, 35,586 sequences). For each protein expression experiment, one combined database search was performed where the data files from all 20 independent MS fraction analyses were searched collectively as a single input dataset. MS/MS spectra searches incorporated fixed modifications of carbamidomethylation of cysteine and iTRAQ (8plex) modification of lysines and peptide N-termini. Variable modification of oxidized methionine was allowed. A decoy database search strategy was used to estimate the false discovery rate (FDR), defined as the percentage of decoy proteins identified

against the total protein identification. The FDR was calculated on the fly using Mascot's 'Automatic Decoy Search' algorithm. During the search, every time a protein sequence from the target database is tested, a reverse decoy sequence of the same length and same average amino acid composition with the target database is automatically generated and tested (2). Before filtering the protein expression data, the Mascot peptide ion score corresponding to an FDR level of <1% in each search was determined in Proteome Discoverer. Peptide spectral matches below this cutoff ion score were discarded from subsequent analysis. After application of the above filter criteria, the estimated FDR value was <1% (at the protein level) for each of the technical replicates analyzed (n=2), indicating a high reliability in the proteins identified. Only peptides that could be ascribed to a unique protein were considered for relative quantitation, excluding those common to other isoforms or proteins of the same family. Proteins were identified on the basis of having at least two peptides with an ion score above 99% confidence. Identified peptides were further excluded from quantitative analyses if 1) the peaks corresponding to the iTRAQ labels were not detected or 2) the same peptide sequence was shared by multiple proteins. Peptide summaries were exported from Proteome Discoverer and isotope correction and relative quantification were calculated as follows. Quantitative abundances of proteins were first computed from iTRAQ reporter ion intensities at the peptide level. To correct for slight variations in the amount of sample in each of the iTRAQ channels, the global median of the relative iTRAQ channel ratios in the total dataset were identified and these ratios were then used to normalize the iTRAQ values. A relative fold change for a given peptide was determined relative to the mean of all iTRAQ channels for that specific peptide (*i.e.*, mean normalized

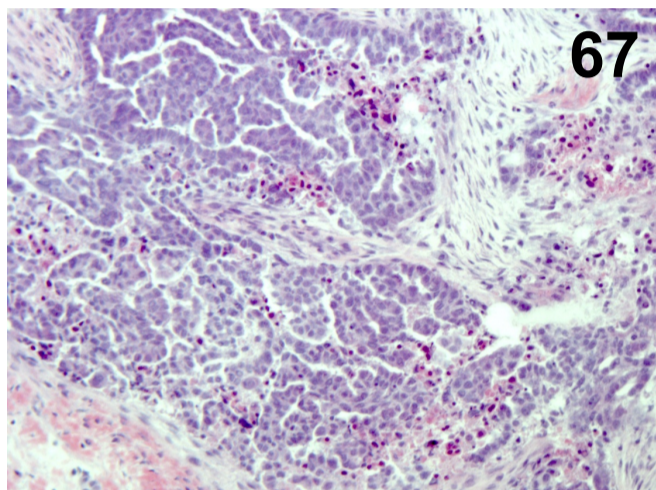
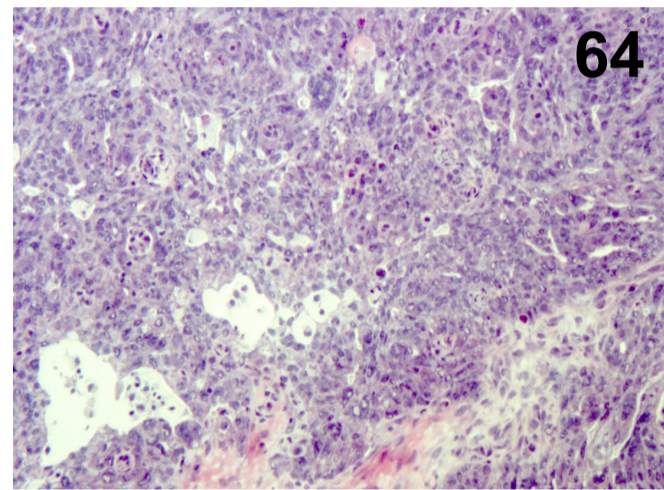
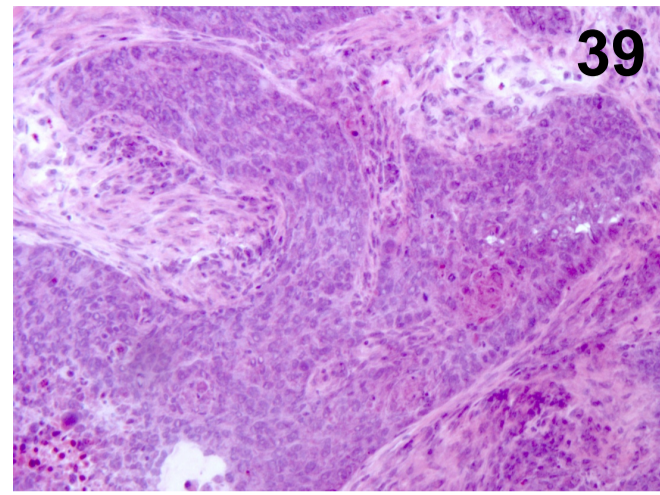
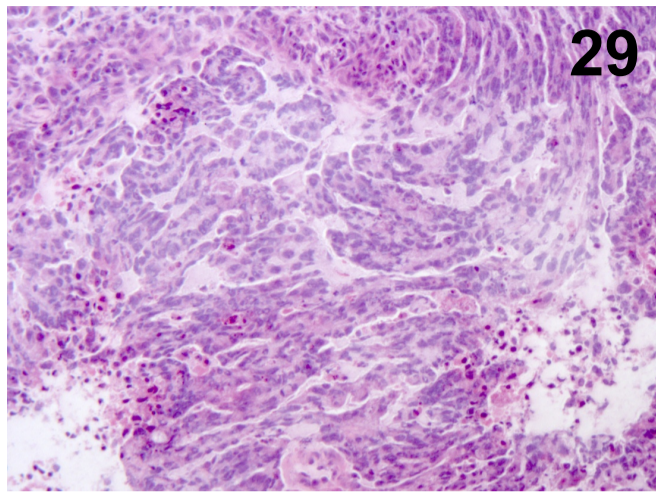
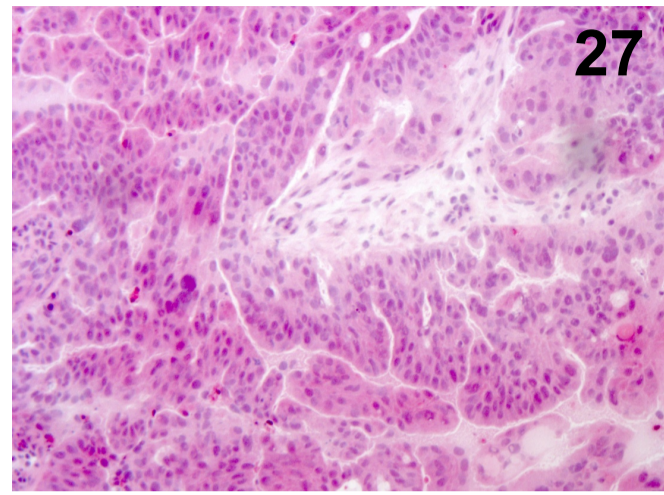
$113 = 113 / ((113 + 114 + 115 + 116 + 117 + 118 + 119 + 121) / 8)$). The normalized iTRAQ value was transformed to \log_2 scale. Quantitative protein expression values were calculated from the mean of all peptide values corresponding to the same protein. The final iTRAQ value for a given protein was calculated from the mean of technical replicate measurements (n=2). For proteins detected in both technical replicates, the standard deviation (s.d.) of each iTRAQ value were calculated from the pair of replicate measurements. The total list of peptides and proteins identified and quantified can be found in **Supplementary Table 5**.

REFERENCES

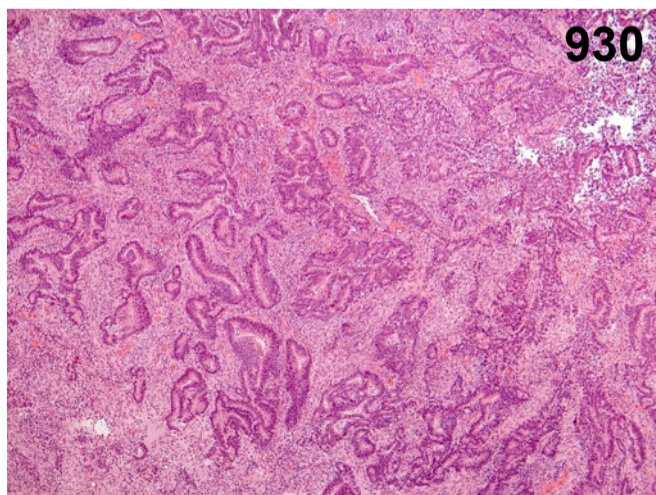
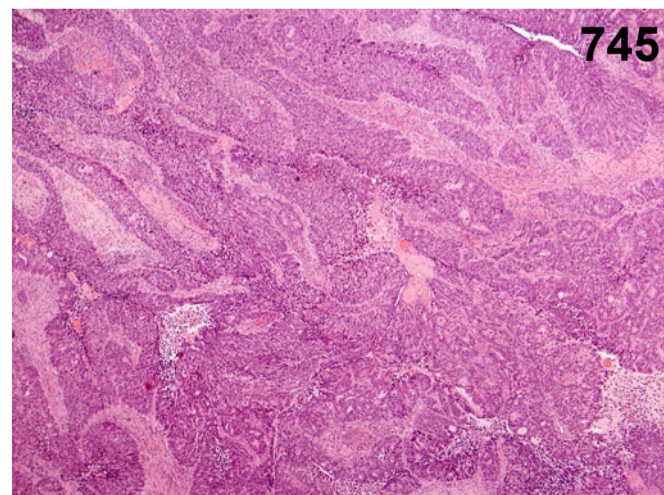
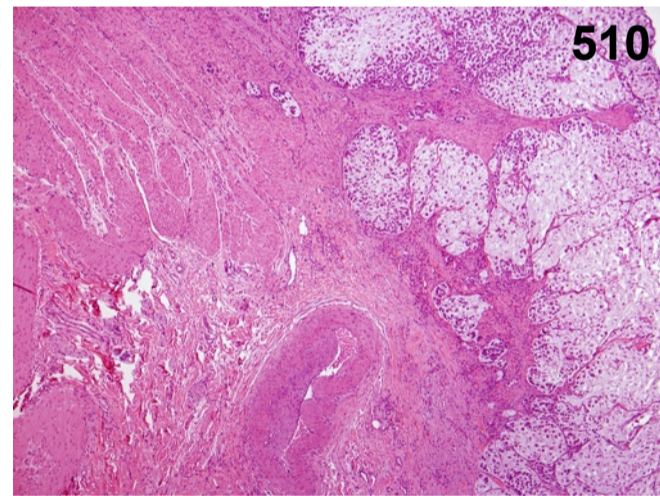
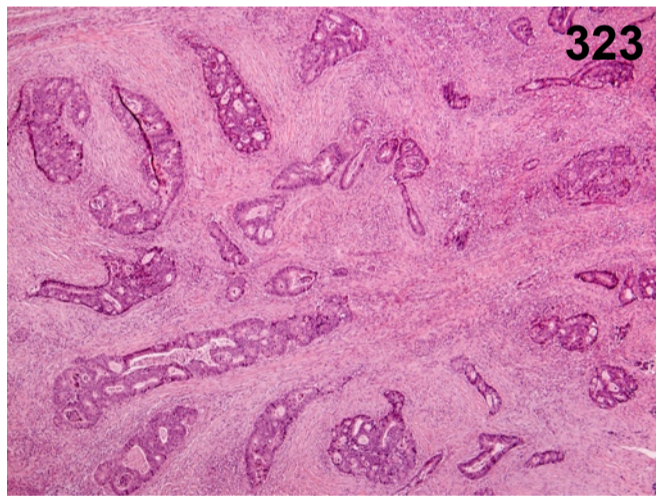
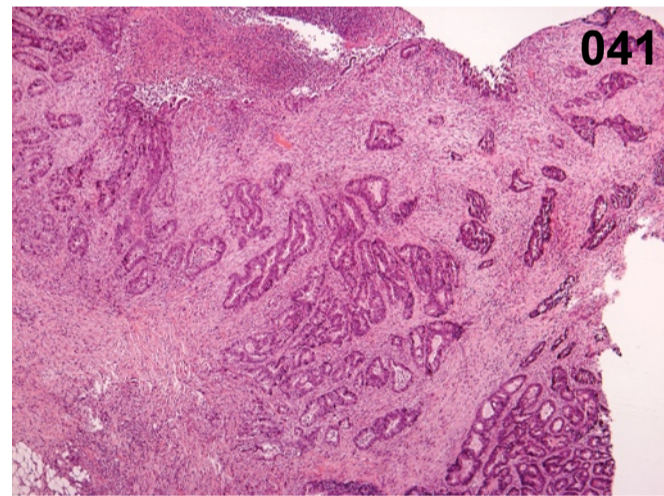
1. Mertins P, Yang F, Liu T, Mani DR, Petyuk VA, Gillette MA, et al. Ischemia in tumors induces early and sustained phosphorylation changes in stress kinase pathways but does not affect global protein levels. *Molecular & Cellular Proteomics*. 2014.
2. Wang G, Wu WW, Zhang Z, Masilamani S, Shen R-F. Decoy methods for assessing false positives and false discovery rates in shotgun proteomics. *Anal Chem*. 2009;81:146–59.

Supplementary Figure 1 Histopathology images of tumors used in ischemia time-course and spatial heterogeneity experiments. Shown are hematoxylin and eosin images of representative sections from **(a)** high-grade serous ovarian carcinoma tissue specimens (10x magnification) and **(b)** colon adenocarcinoma tissue specimens (4x magnification). Sample identifiers consistent with those used in the study are overlaid on each image.

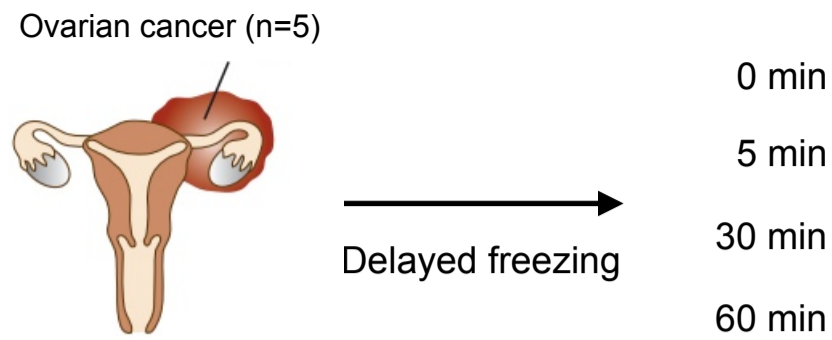
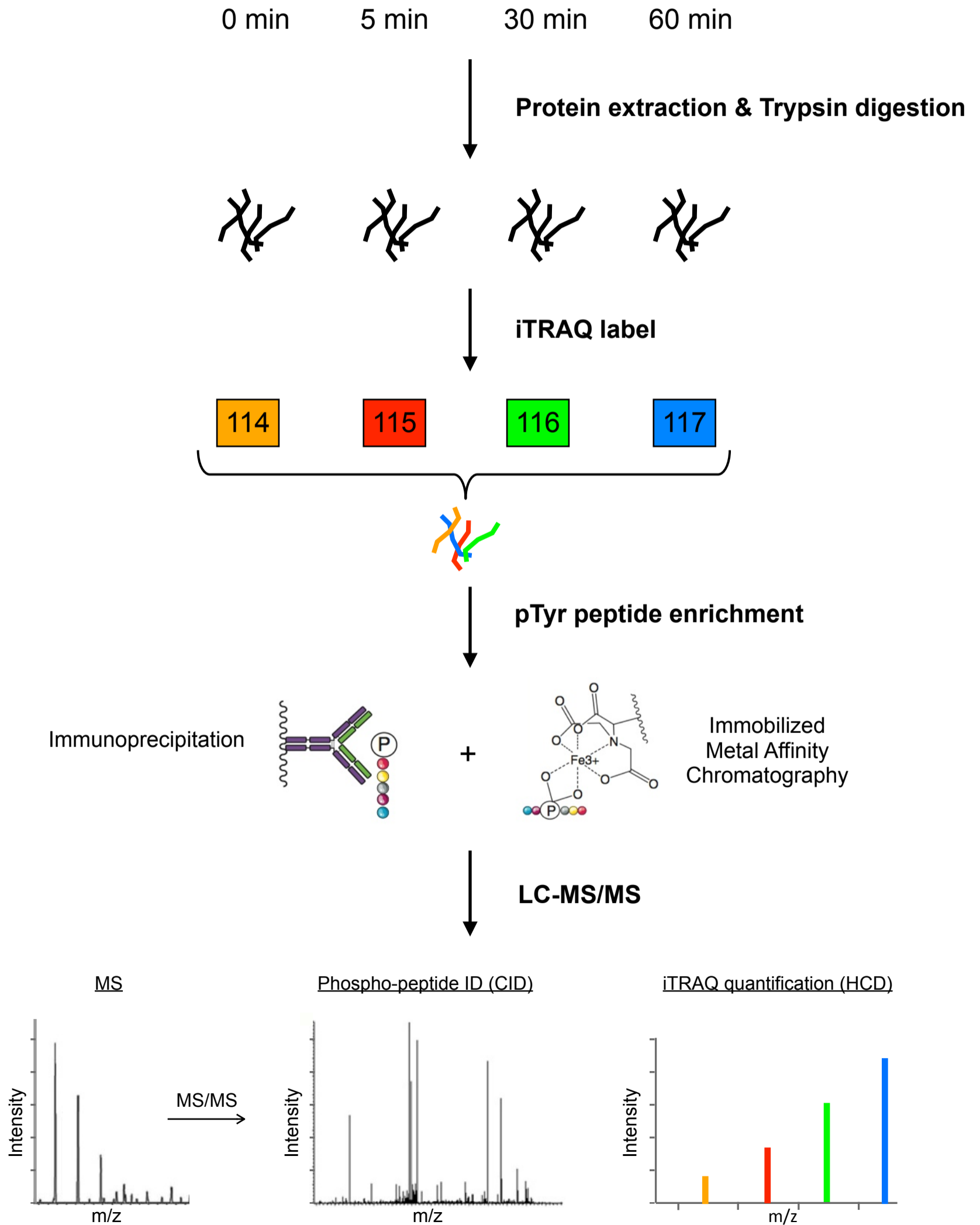
a



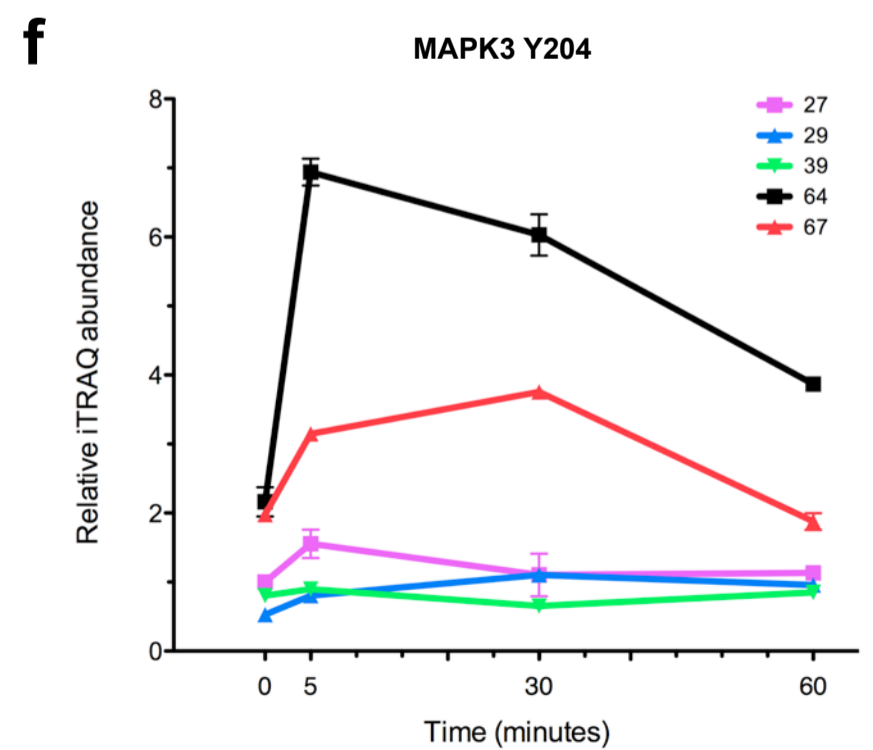
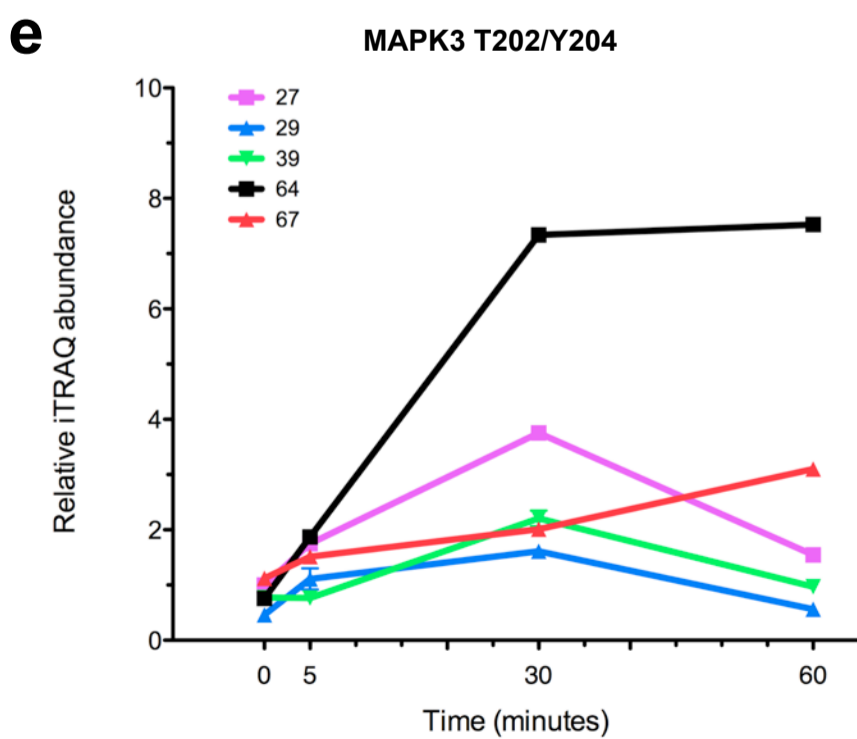
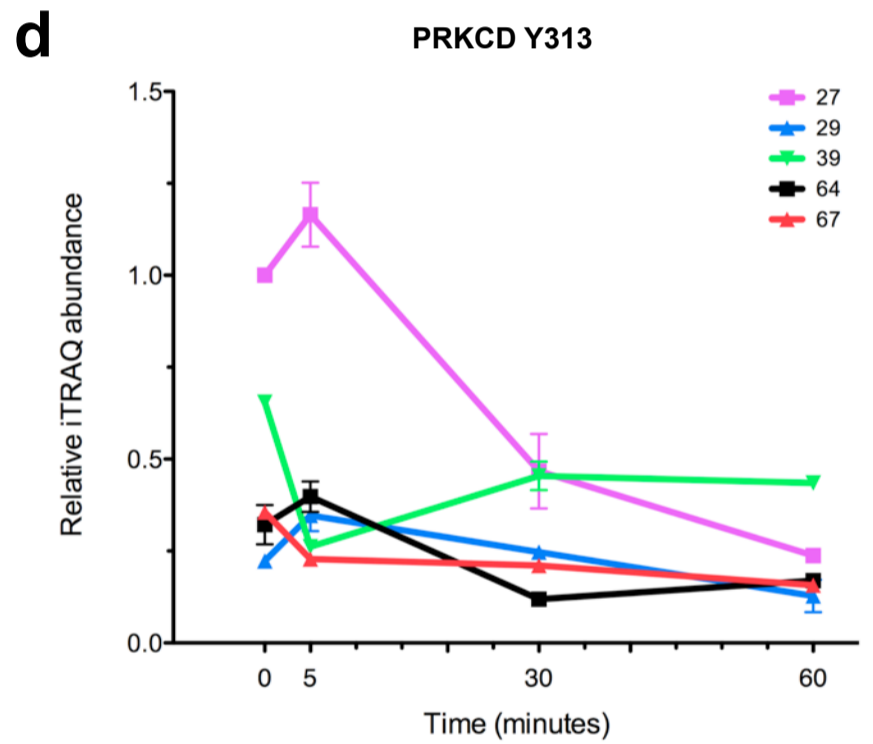
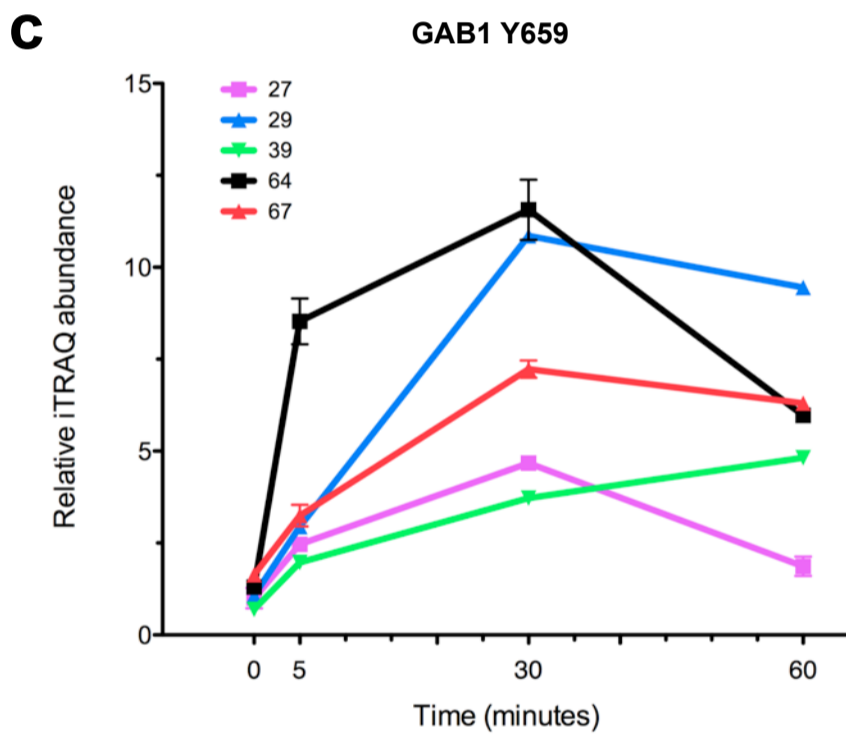
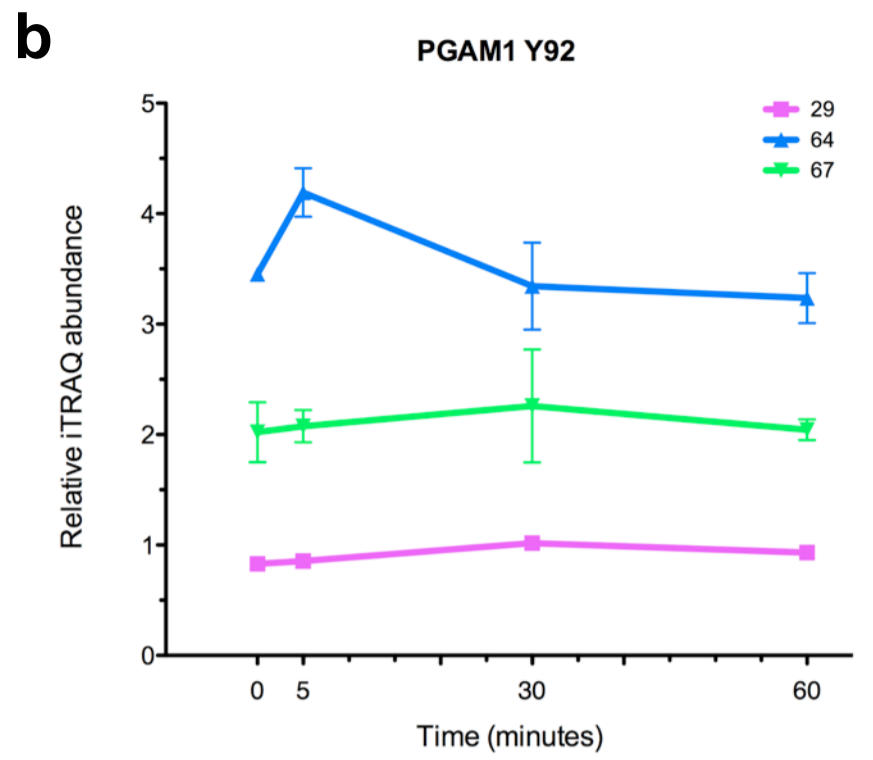
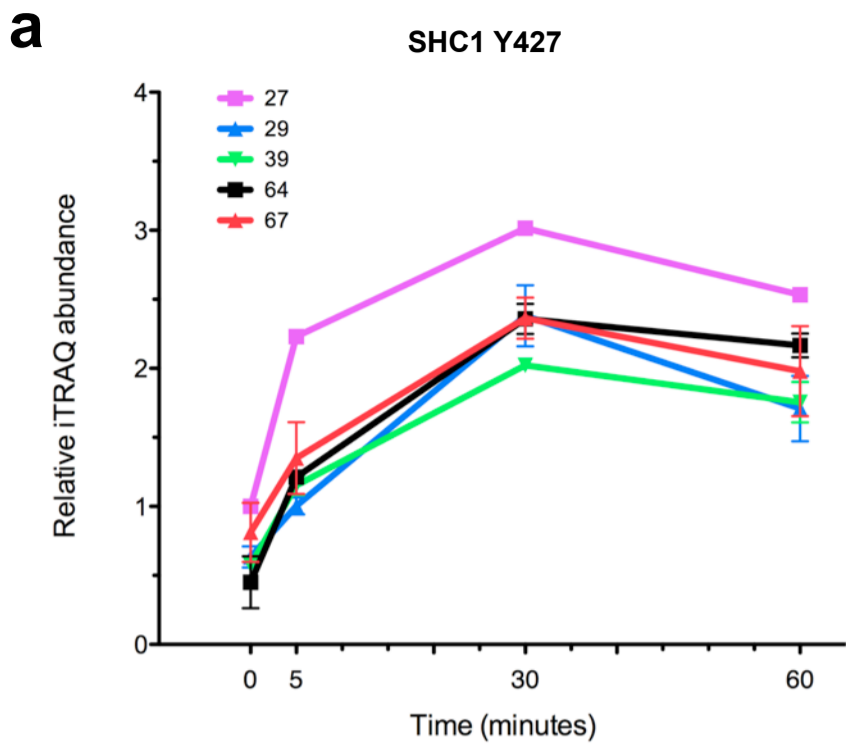
b



Supplementary Figure 2 Schematic overview of ovarian tumor ischemia time-course experiment. **(a)** Ovarian tumors were resected from patients, divided into 4 equal sized parts and frozen after 0, 5, 30, and 60 min of cold ischemia. **(b)** Four ischemia time-points of each ovarian tumor were run in a separate 4-plex analysis per patient, and 2 technical replicates were completed per patient. Samples were homogenized to extract proteins and then digested into peptides with trypsin protease. Peptides were differentially labelled with iTRAQ (Isobaric Tags for Relative and Absolute Quantification) chemical mass tags and mixed together for simultaneous analysis. pTyr peptides were enriched using pY immunoprecipitation (IP) followed by immobilized metal affinity chromatography (IMAC). The enriched phospho-peptides were analyzed by LC-MS/MS to allow phosphopeptide identification from sequence specific fragment ions as well as pTyr quantification at each ischemia time-point from the relative amounts of the iTRAQ mass tags. CID: collision-induced dissociation; HCD: higher-energy c-trap dissociation.

a**b**

Supplementary Figure 3 Distinct inter-patient ischemia regulated temporal dynamics are observed. **(a, b)** Examples of select pTyr sites are shown where the type of temporal trend is unaffected by the basal phosphorylation level. **(c,d)** In some cases, the magnitude or type of response observed is dependent on the initial phosphorylation level at time of resection. **(e,f)** In other cases, the same protein can exhibit different dynamics depending on which pTyr site is measured. Colored lines represent relative inter-patient phosphorylation levels, mean \pm s.d. of technical replicates is shown. Temporal data values shown are derived from independent patient datasets and normalized with t=0 value measured from '0 min' timepoint analysis. The full list of t=0 normalized pTyr sites can be found in Supplemental Table 2.

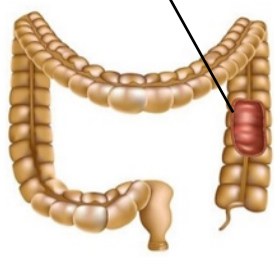


Supplementary Figure 4 Similar ischemia response temporal patterns are observed across ovarian tumors. Subplots signify groups of pTyr sites with similar quantitative trends across time (x-axis) according to affinity propagation analysis. Solid lines denote the temporal trends of individual pTyr sites. Mean \log_2 temporal values relative to $t=0$ min are shown. Exemplar pTyr site of each cluster shown in blue. The full list of pTyr sites within each plot and the results of each individual tumor affinity propagation analysis can be found in Supplemental Table 3.

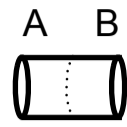
Supplementary Figure 5 Schematic overview of the colon tumor spatial heterogeneity and ischemia time-course experiment. **(a)** Colon tumors were resected from patients and core biopsy punches were collected and frozen after 0, 10, 30, and 60 min of cold ischemia. Each biopsy punch was split in half to generate a pair of spatially distinct samples at each timepoint. **(b)** Eight ischemia time-points of each colon tumor were run in a separate 8-plex analysis per patient, and 2 technical replicates were completed per patient. Samples were homogenized to extract proteins and then digested into peptides with trypsin protease. Peptides were differentially labelled with iTRAQ (Isobaric Tags for Relative and Absolute Quantification) chemical mass tags and mixed together for simultaneous analysis. pTyr peptides were enriched using pY immunoprecipitation (IP) followed by immobilized metal affinity chromatography (IMAC). The enriched phosphopeptides were analyzed by LC-MS/MS to allow phosphopeptide identification from sequence specific fragment ions as well as pTyr quantification at each ischemia time-point from the relative amounts of the iTRAQ mass tags. CID: collision-induced dissociation; HCD: higher-energy c-trap dissociation.

a

Colon cancer (n=5)



Biopsy punch



Delayed freezing

0 min
10 min
30 min
60 min

b

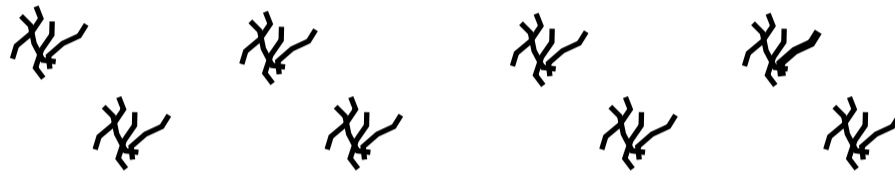
0 min
A B

10 min
A B

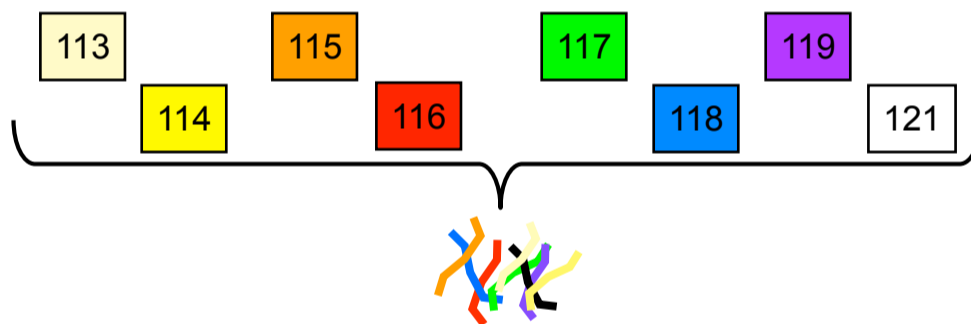
30 min
A B

60 min
A B

Protein extraction & Trypsin digestion

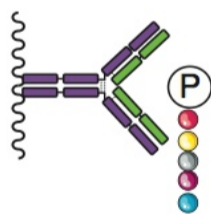


iTRAQ label

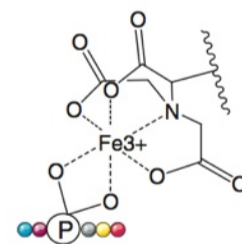


pTyr peptide enrichment

Immunoprecipitation



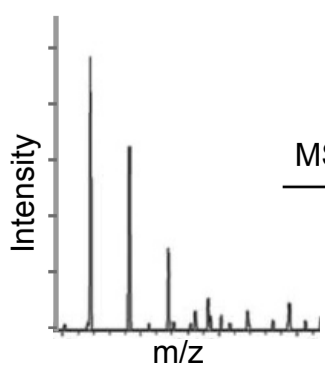
+



Immobilized
Metal Affinity
Chromatography

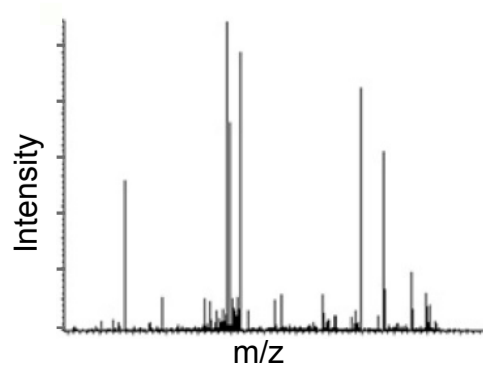
LC-MS/MS (Orbitrap Elite)

MS

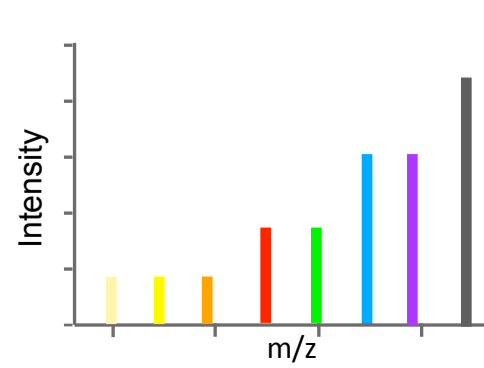


MS/MS

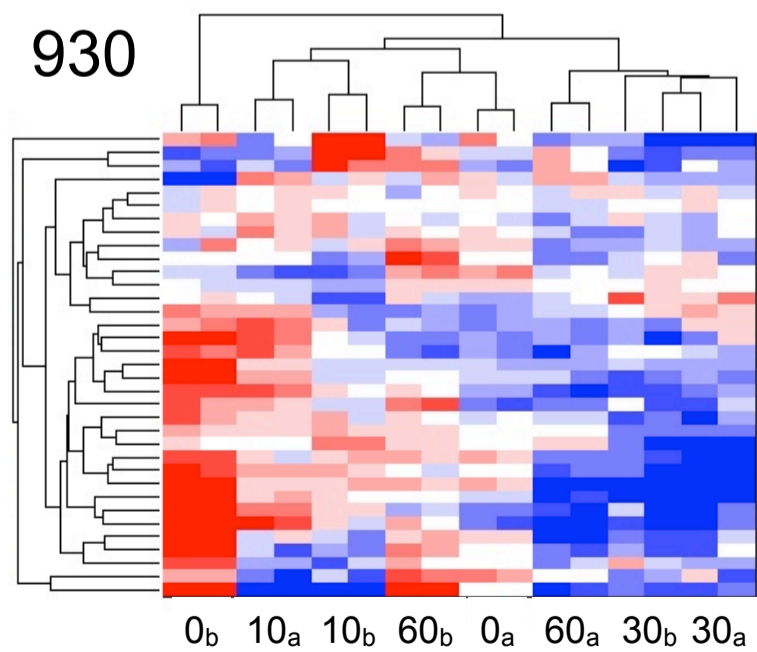
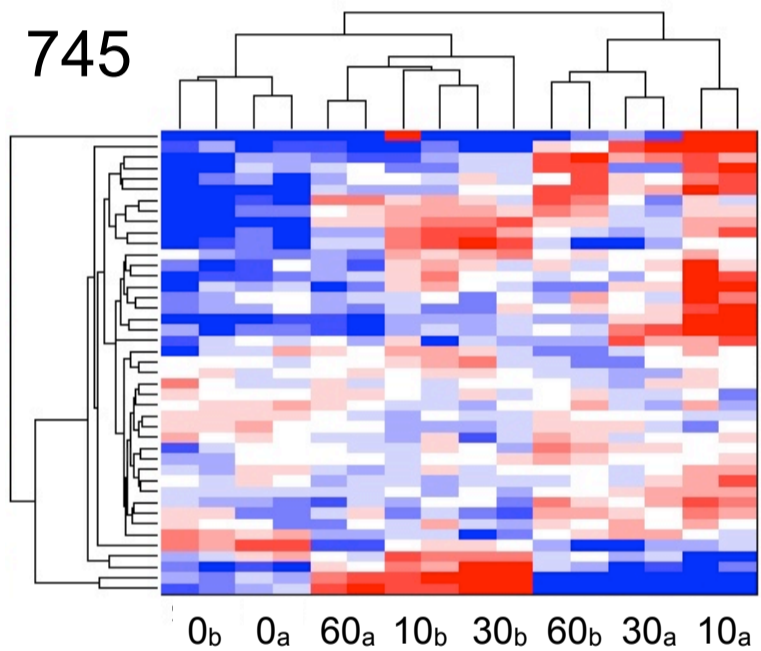
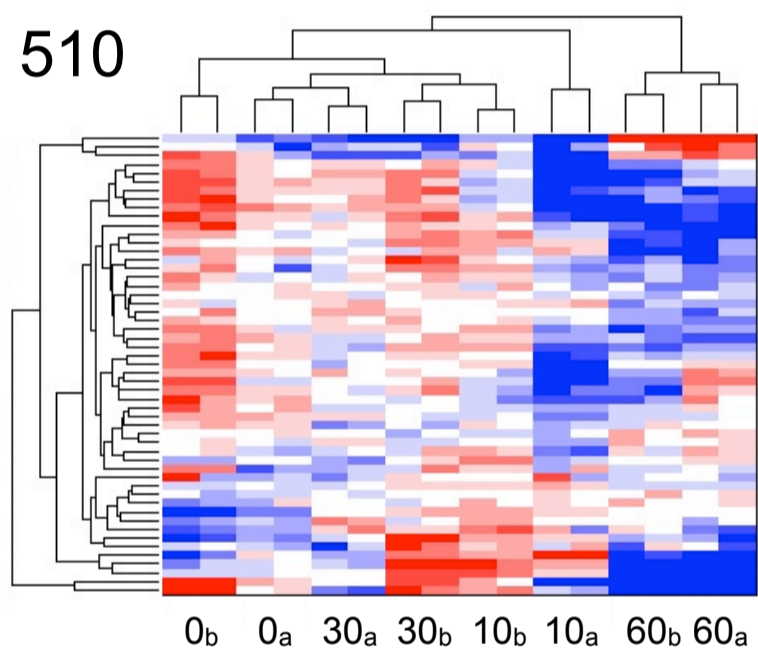
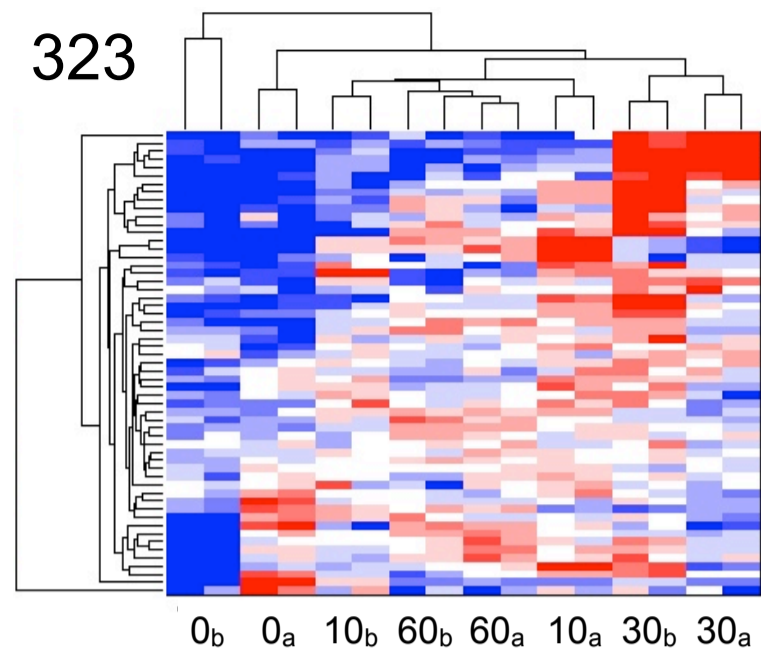
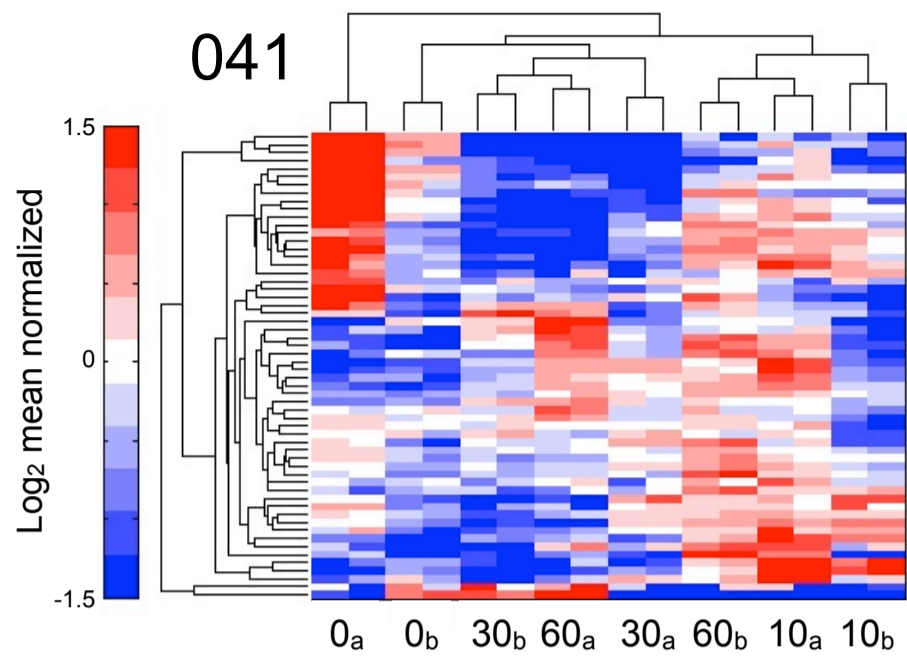
Phospho-peptide ID (CID)



iTRAQ quantification (HCD)



Supplementary Figure 6 Spatial phosphorylation heterogeneity in colons tumors cannot be attributed solely to technical measurement error. Separate unsupervised hierarchical-clustered heatmaps represent the grouping of technical replicate measurements for each patient-derived colon tumor. Note the similarity between technical replicates at any given measurement. Patient identifier shown to top left of each heatmap. Rows indicate mass spectrometry-derived quantitative levels of pTyr sites in \log_2 mean normalized scale. Onset of saturated color in the heatmaps corresponds to changes ≥ 2 -fold from the mean (red, increasing; blue, decreasing).



Supplementary Figure 7 Weak correlations and minimal shared covariance between spatially proximal colon tumor samples. Pearson correlation analysis was used to quantify the direction and magnitude of correlation among the spatially distinct colorectal tumor samples. Data points presented in each plot are the \log_2 mean-centered value for a given pTyr site between paired spatially-distinct samples at the indicated timepoints. r =Pearson correlation coefficient; 95% CI=95% confidence interval of r ; P =two-tailed p-value.

Patient 041

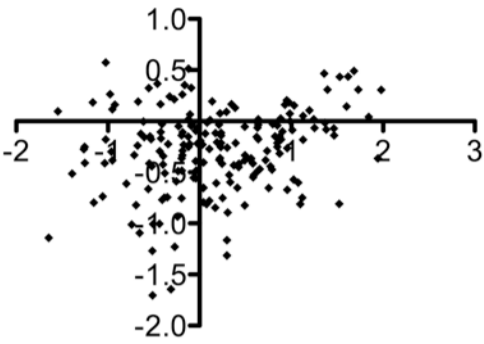
Patient 510

Patient 745

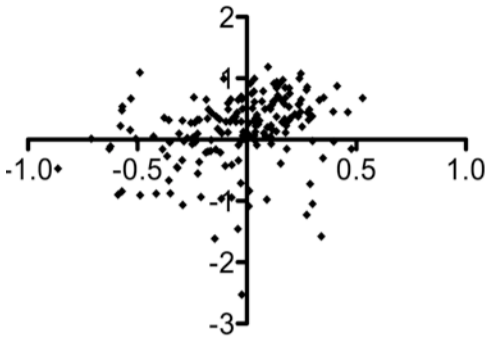
Patient 930

0_a VS 0_b

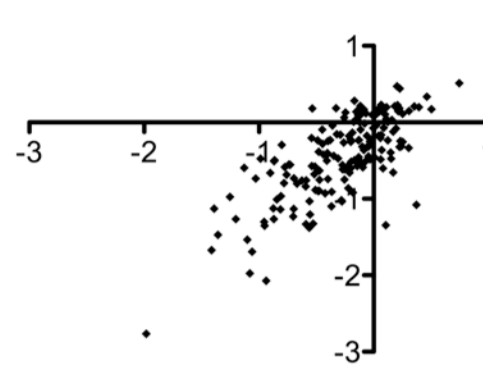
$r = 0.2347$
95% CI= 0.09552 to 0.3649
 $P = 0.0011$
 $r^2 = 0.05509$



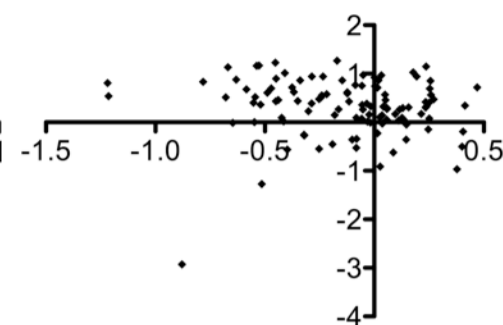
$r = 0.2708$
95% CI= 0.1305 to 0.4005
 $P = 0.0002$
 $r^2 = 0.07334$



$r = 0.7378$
95% CI= 0.6614 to 0.7991
 $P < 0.0001$
 $r^2 = 0.5444$

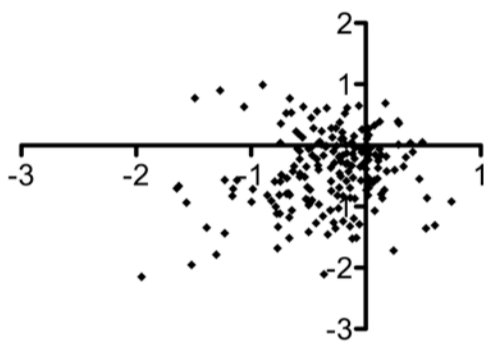


$r = -0.06440$
95% CI= 0.09552 to 0.3649
 $P = 0.5059$
 $r^2 = 0.004147$

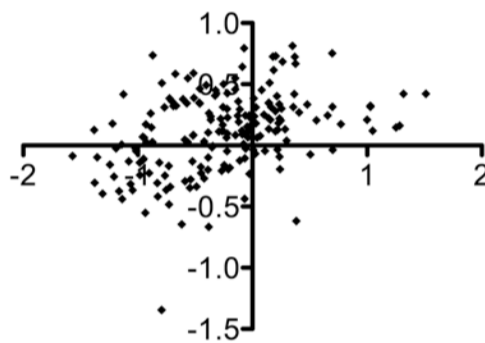


10_a VS 10_b

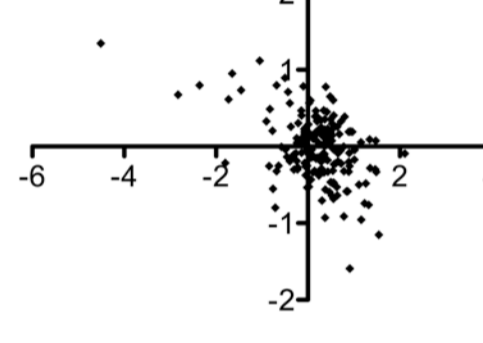
$r = 0.1714$
95% CI= 0.02978 to 0.3064
 $P = 0.0180$
 $r^2 = 0.02939$



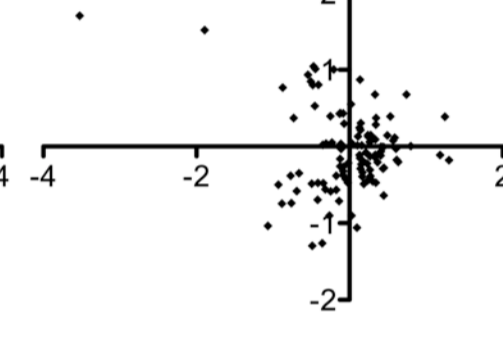
$r = 0.3859$
95% CI= 0.2547 to 0.5032
 $P < 0.0001$
 $r^2 = 0.1489$



$r = -0.4661$
95% CI= -0.5754 to -0.3406
 $P < 0.0001$
 $r^2 = 0.2173$

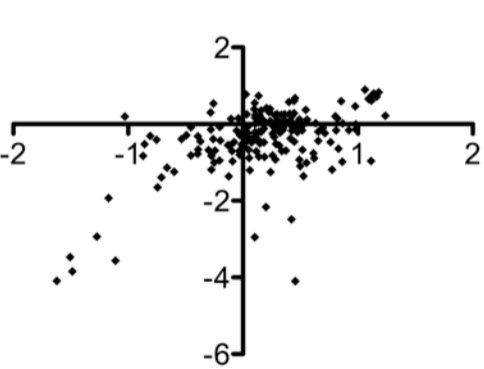


$r = -0.2047$
95% CI= -0.3783 to -0.01719
 $P = 0.0328$
 $r^2 = 0.04189$

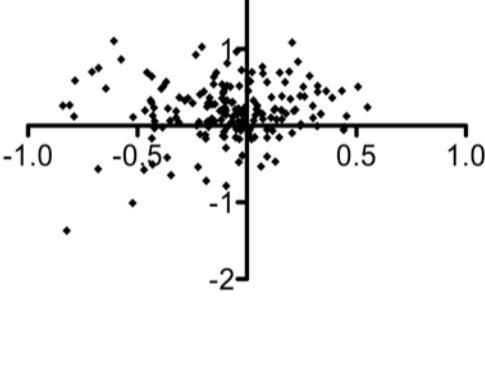


30_a VS 30_b

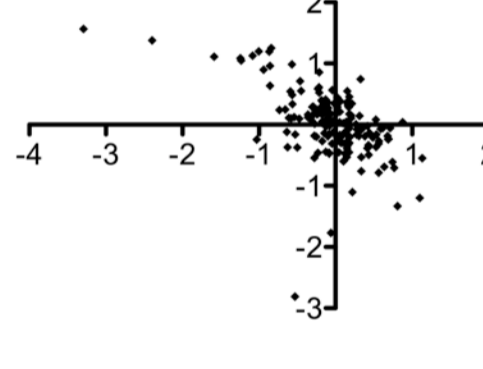
$r = 0.5314$
95% CI= 0.4208 to 0.6264
 $P < 0.0001$
 $r^2 = 0.2824$



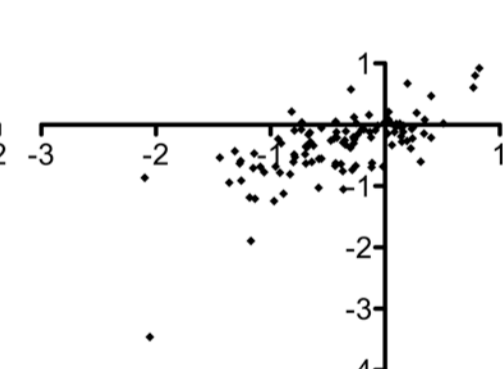
$r = 0.09326$
95% CI= -0.05295 to 0.2356
 $P = 0.2105$
 $r^2 = 0.008698$



$r = -0.5787$
95% CI= -0.6703 to -0.4698
 $P < 0.0001$
 $r^2 = 0.3349$

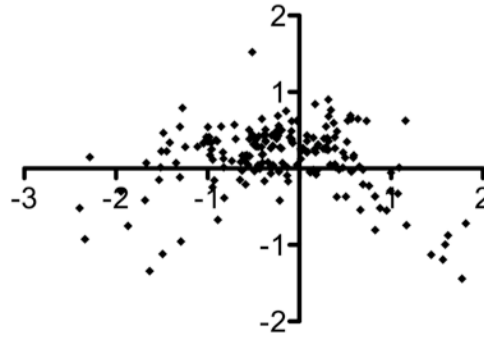


$r = 0.6827$
95% CI= 0.5668 to 0.7721
 $P < 0.0001$
 $r^2 = 0.4661$

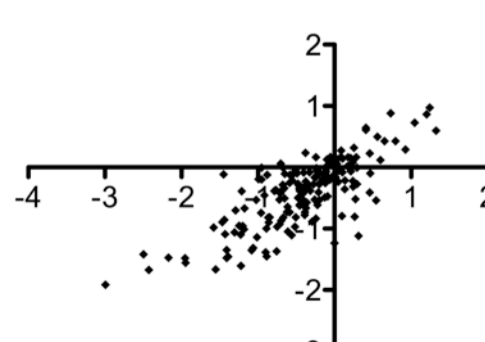


60_a VS 60_b

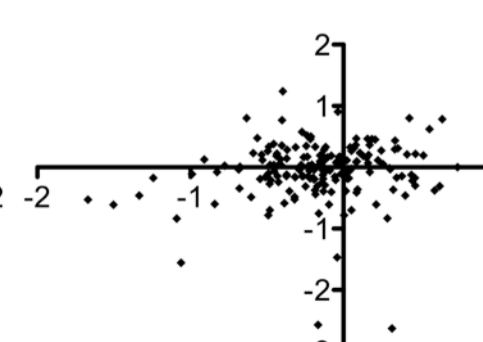
$r = -0.1196$
95% CI= -0.2576 to 0.02322
 $P = 0.1004$
 $r^2 = 0.01430$



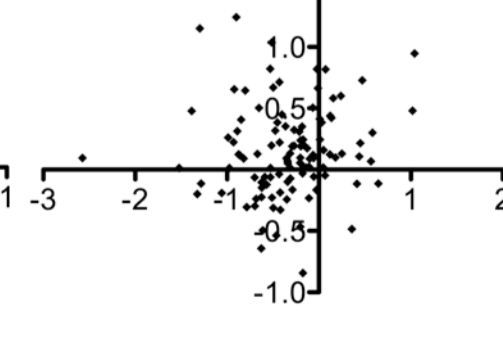
$r = 0.7761$
95% CI= 0.7109 to 0.8281
 $P < 0.0001$
 $r^2 = 0.6023$



$r = 0.1351$
95% CI= -0.01447 to 0.2787
 $P = 0.0765$
 $r^2 = 0.01824$

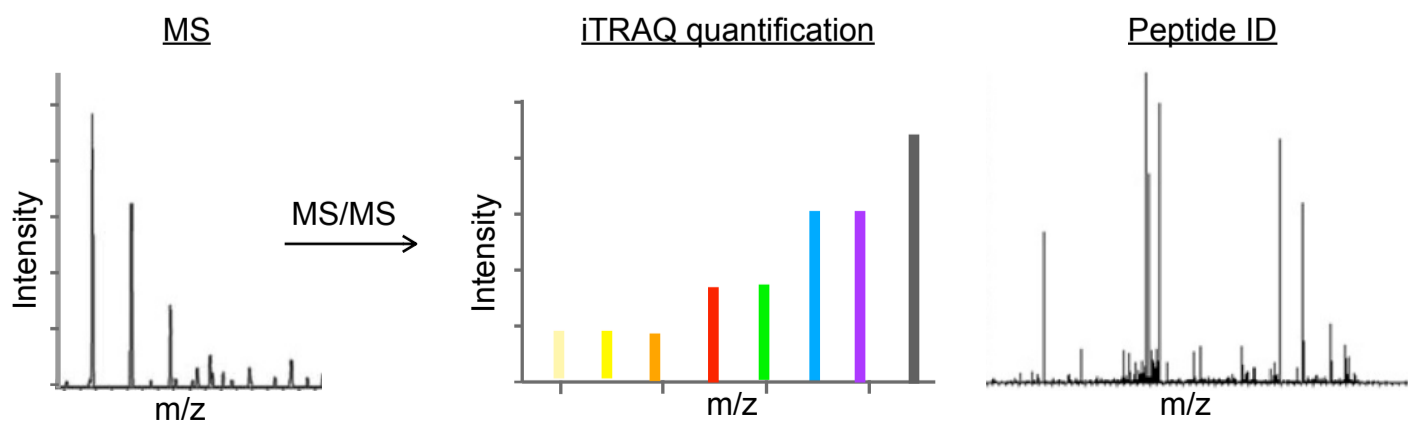
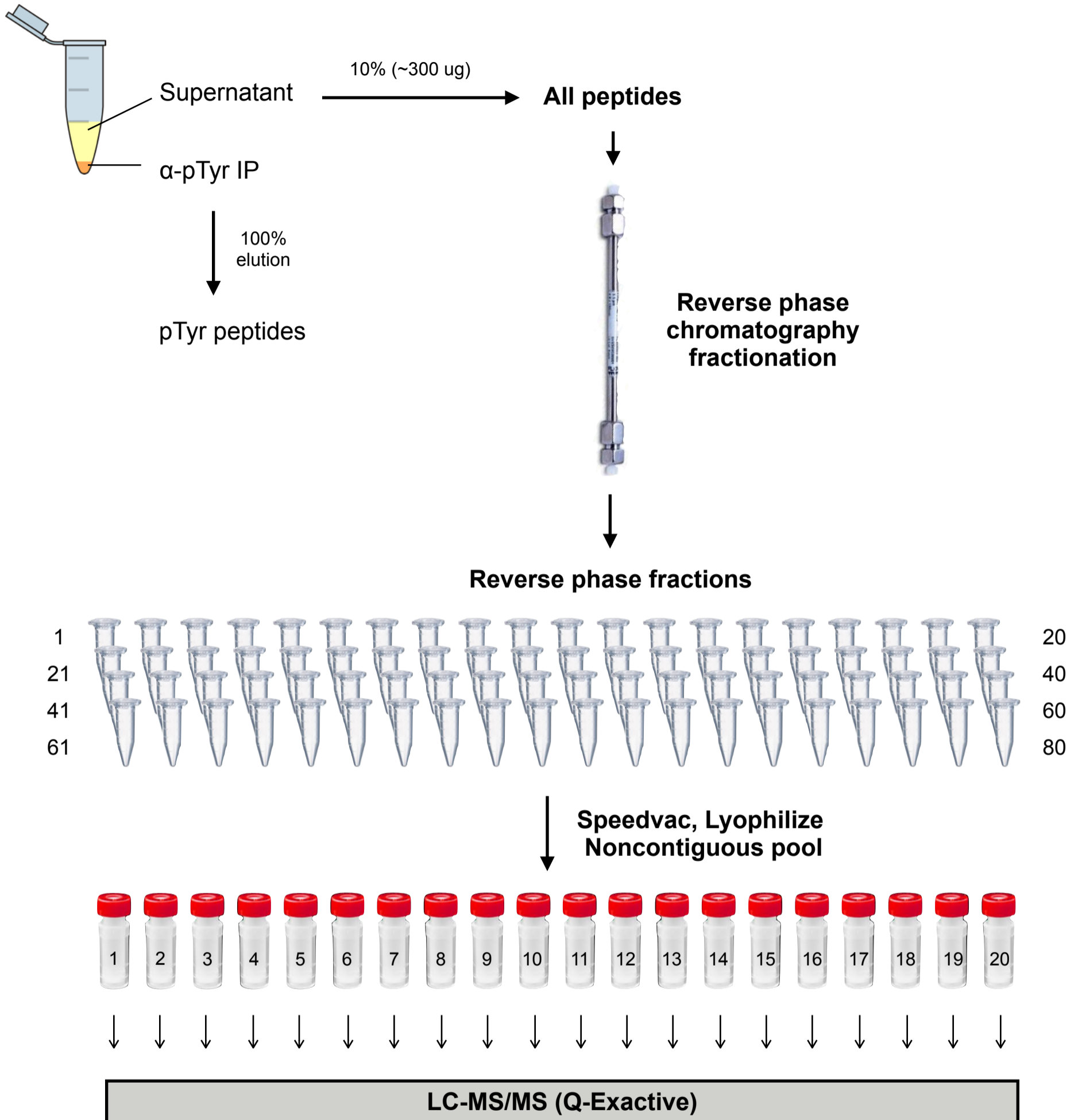


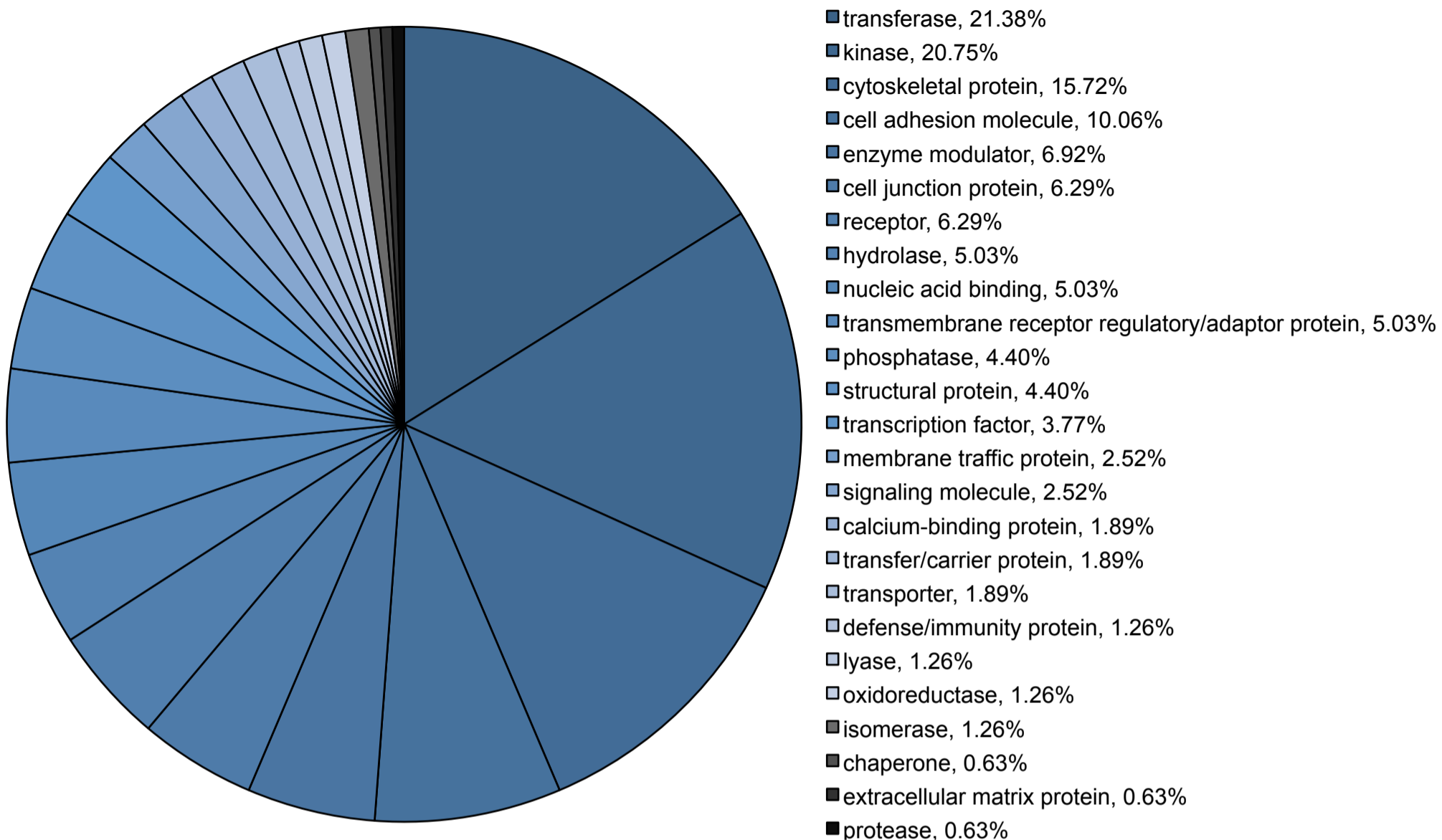
$r = 0.08564$
95% CI= -0.1042 to 0.2694
 $P = 0.3759$
 $r^2 = 0.007335$



Supplementary Figure 8 Schematic overview of the colon tumor protein expression profiling experiment. An aliquot of iTRAQ labeled peptides from each colorectal tumor pTyr IP supernatant was collected and separated off-line to reduce sample complexity. A total of 80 peptide fractions were collected per sample. Lyophilized peptides fractions were then reconstituted and pooled together in a non-contiguous fashion (ie. Fraction 1+21+41+61, etc.) to generate 20 final fractions. Each of the 20 final fractions underwent an independent LC-MS/MS analysis to provide protein identification from sequence specific fragment ions and quantification from the relative amounts of the iTRAQ mass tags. A total of two technical process replicates were completed per patient.

iTRAQ labeled colon tumor peptides





Supplementary Figure 9 Delayed freezing of tumors affects pTyr sites involved in numerous pathways and processes. PANTHER classification was used to annotate the protein classes represented by ischemia-regulated pTyr sites from the union of the ovarian and colon tumor datasets. Listed are the PANTHER protein class and corresponding percentage of sites from the combined colon and ovarian datasets in each category. The final four classes (shown in shades of gray) are specific to the colon dataset and not represented in the ovarian dataset.